On the γ-Phase of Isotactic Polypropylene

Ralf Thomann, Chun Wang, Jörg Kressler,* and Rolf Mülhaupt

Freiburger Materialforschungszentrum und Institut für Makromolekulare Chemie, Albert-Ludwigs-Universität Freiburg, Stefan-Meier-Strasse 21, D-79104 Freiburg/Brsg., Germany

Received December 21, 1995; Revised Manuscript Received July 25, 1996[⊗]

ABSTRACT: The crystalline morphology of a relatively high molecular weight isotactic polypropylene (i-PP) (M_w = 18000 g/mol) with well-defined regio- and stereoirregularities is studied by means of atomic force microscopy (AFM), wide-angle X-ray scattering (WAXS), small-angle X-ray scattering (SAXS), and light microscopy. This i-PP crystallizes under certain crystallization conditions nearly exclusively in the γ-modification. The growth of the γ-phase is often influenced by the initial growth of the α-phase, but also the neat γ-phase is observable. The formation of the γ-phase can be related to stereo- and regioirregularities in the polymer chain caused by the polymerization mechanism using metallocene catalysts. WAXS measurements show that at large supercoolings the formation of α-phase i-PP is preferred, whereas at low supercoolings this sample crystallizes nearly exclusively in the γ-modification. Light microscopy and AFM reveal for the γ-phase i-PP morphologies different from the well-known spherulites formed by the α- or β-modification. However, it can be shown that the morphology development of γ-phase i-PP can be widely influenced by very small amounts of α-phase i-PP. A lamella thickness of about 4 nm and a long period of 12 nm of γ-phase i-PP isothermally crystallized at 100 °C are obtained from SAXS measurements. At very low supercoolings, supermolecular structures of the neat γ-modification are formed in competition with mixed (α and γ) morphologies. In thin films the neat γ-modification shows network structures, which are formed by triangular entities. Etched bulk samples reveal columns with a rectangular cross-section which are densely packed. On the molecular scale, the surface topography of the flat-on extended chain lamellae with periodic distances of rows of methyl groups of 3.6 Å is measured. This value is in excellent agreement with the distance of the methyl group rows on the crystallographic (010) plane according to the nonparallel chain packing model by Brückner and Meille.

Introduction

The crystallization behavior of isotactic polypropylene (i-PP) is very complex. Numerous groups have aimed their research on a better understanding of the different crystal modifications (α, β, γ, and smectic).[1−7] At atmospheric pressure the γ-modification is commonly observed as a minor constituent in bulk-crystallized i-PP.[2,8] Large contents of the γ-modification are obtained when i-PP is crystallized at elevated pressures[9,10] or when very low molecular weight samples (between 1000 and 3000 g/mol) are used.[11−14] These samples can be produced by thermal degradation of high molecular weight i-PP.[15,16] Also random copolymers of propene with 2.5−20 wt % of other 1-olefins may crystallize preferably in the γ-modification.[17−22] More recently, it has been shown that high molecular weight i-PP samples prepared by employing metallocene catalyst systems may tend to crystallize in the γ-modification.[23,24] Similar to propene copolymers with 1-olefins, the steric irregularities of these samples have been proposed to be responsible for the formation of the γ-modification.[23] Calculations of the packing energies of the γ- and α-modifications show that the γ-modification should be slightly more stable than the α-modification.[25,26] The orthorhombic unit cell of the γ-modification is formed by bilayers composed of two parallel helices.[27−29] The direction of the chain axis in adjacent bilayers is tilted with an angle of 80°.[27−29] This is a unique packing arrangement for polymers but has been known e.g. for fatty acids.[30] Lotz et al. have made a remarkable work to support this nonparallel chain packing model. They pointed out that the electron diffraction experiments on a flat-on γ-phase single crystal resulted in the same patterns after clockwise 40° rotation and anticlockwise 40° rotation, which corresponds to an angle of 80° between the double layers of helices arranged in the unit cell.[15]

This study deals with the observation of the morphology of i-PP, crystallized mainly in the γ-modification. Wide-angle X-ray scattering (WAXS) measurements are used for the determination of the ratio of α- to γ-modification as a function of the crystallization temperature. The lamella thickness and the long period are determined by small-angle X-ray scattering (SAXS). Light microscopy and atomic force microscopy (AFM) are employed for the investigation of the neat γ-modification and the influence of small amounts of α-phase i-PP on the morphology development of the γ-phase.

Experimental Section

Material. The i-PP sample under investigation is synthesized using the homogeneous catalyst system *rac*-(ethylene)-bis(4,5,6,7-tetrahydroindenyl)zirconium(IV) dichloride/MAO. This i-PP has an M_w value of 18 000 g/mol and M_w/M_n of 1.6. These data are obtained by SEC of i-PP dissolved in 1,2,4-trichlorobenzene at 140 °C. An IR detector is used and the calibration is done with narrow molecular weight i-PP samples characterized by light scattering. The sample contains 81.5% of mmmm pentads, 8.8% of mmmr pentads, 0.1% of rmmr pentads, 6.5% of mmrr pentads, 0.2% of rrrm pentads, and 2.9% of mrrm pentads, determined by ^{13}C NMR. rmrr, mrmm, and rmrm pentads are not detectable.[31] The average length of isotactic chain segments is about 22.4 monomeric units, i.e. a length of 4.85 nm when arranged in a 3_1 helix. Besides the distribution of pentads, defect structures caused by 1−3 insertion are formed and equally distributed on all chains.[31]

Sample Preparation. The samples used to study the crystalline morphology by light microscopy are prepared by melting the powder of the as-prepared and dried polymer between two cover glasses. The layer thickness between the glasses is about 30−50 μm. The samples are held for 10 min at 160 °C and then quenched to crystallization temperature

* To whom correspondence should be addressed.

[⊗] Abstract published in *Advance ACS Abstracts,* November 1, 1996.

S0024-9297(95)01885-7 CCC: $12.00 © 1996 American Chemical Society

at a rate of 30 °C/min. The bulk sample (thickness of about 2 mm) is prepared in a vacuum oven after cooling from 160 to 120 °C and keeping it there for 1 week. The single crystals of γ-phase i-PP are prepared by casting a dilute solution of i-PP in *n*-heptane (0.01 wt %) on a clean cover glass. The solvent is evaporated at room temperature and then dried for several days in a vacuum oven. Finally, the sample is heated to 160 °C and held at this temperature for 10 min, cooled at a rate of 0.1 °C/min to 120 °C, and isothermally crystallized at this temperature for 3 days.

Light Microscopy. The light microscopic investigations are carried out with an Olympus-Vanox AH2 microscope and a Linkam TMS 90 hot stage that allows observation during isothermal crystallization. The light intensity between crossed polarizers is measured with a photocell in the microscope and is then normalized. This means that the constant light intensity after a long crystallization time is taken as 100% and the initial value of the sample in the molten state as 0%.

Atomic Force Microscopy. The prepared films are etched to remove amorphous material from the surface. Only the as-prepared single-crystal aggregates on glass are not etched. The etching reagent is prepared by stirring 0.02 g of potassium permanganate in a mixture of 4 mL of sulfuric acid (95−97%) and 10 g of orthophosphoric acid. The 30−50 μm thick films are immersed into the fresh etching reagent at room temperature and held there for 1 h. In the beginning, the samples are held in an ultrasonic bath for 30 min. For subsequent washings, a mixture of 2 parts by volume of concentrated sulfuric acid and 7 parts of water is prepared and cooled to near the freezing point with dry ice in 2-propanol. The samples are washed successively with 30% aqueous hydrogen peroxide (to remove any manganese dioxide present). Then the samples are washed with distilled water. Each washing was supported with an ultrasonic bath. The AFM experiments are carried out with a Nanoscope III scanning probe microscope (Digital Instruments) at ambient conditions in the height mode.

X-ray Measurements. Samples for WAXS measurements are isothermally crystallized at various temperatures and for various times until a constant degree of crystallinity is reached. The measurements are carried out with a Siemens D500 apparatus. For WAXS and SAXS measurements, Cu Kα radiation of wavelength $\lambda = 0.154$ nm is used. The sample for SAXS measurements is isothermally crystallized at 100 °C. An evacuated Kratky compact camera (Anton Paar K.G.) with an entrance slit of 80 μm is used. The scattering profile is corrected for background scattering and desmeared.[32] The contributions of thermal density fluctuations to the scattering intensity are eliminated by computing the slope of an Is^4 versus s^4 plot at high scattering vectors, $s = (2/\lambda)\sin(\theta/2)$, where I is the scattering intensity and θ is the scattering angle.[33] The Fourier transformation of the scattering curve yields the linear correlation function $K(z)$ defined by[34,35]

$$K(z) = \int_0^\infty 4\pi s^2 I(s) \cos^2 \pi s z \, ds \qquad (1)$$

Results and Discussion

X-ray Measurements. Figure 1 shows WAXS traces of the as-prepared polymer and of the same material isothermally crystallized at 65, 75, and 125 °C. The as-prepared i-PP sample shows exclusively the α-modification. The sample isothermally crystallized at 65 °C still forms mainly the α-modification. The 117 peak of the γ-modification appears only very weak. Increasing crystallization temperatures promote the formation of the γ-modification. The 117 peak increases in the sample crystallized at 75 °C and finally the isothermal crystallization at 125 °C leads nearly exclusively to the γ-modification. The 130 peak of the α-modification appears at this crystallization temperature only very weak.

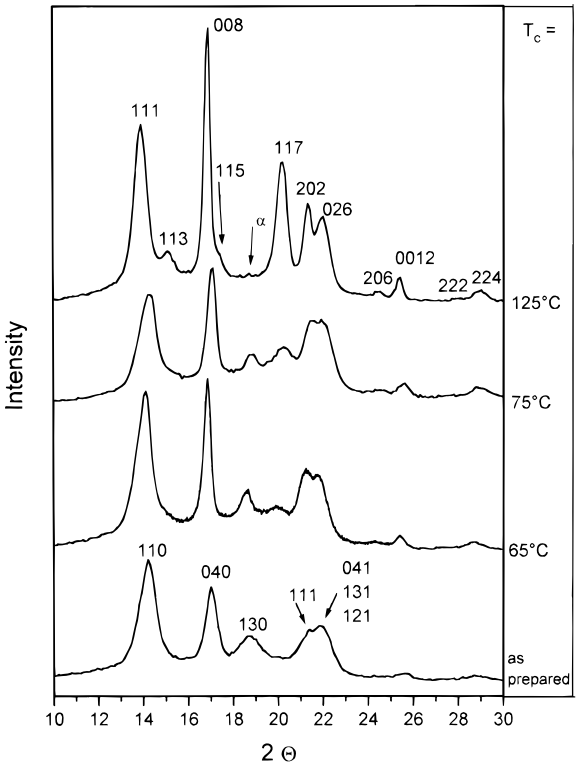

Figure 1. WAXS traces of as-prepared i-PP (bottom) and of samples isothermally crystallized at 65, 75, and 125 °C. The peak assignment of the γ-phase i-PP (top trace) is due to Brückner and Meille[27] and that of the α-phase i-PP is due to Natta et al.[44] The patterns of the as-prepared polymer and the sample isothermally crystallized at 65 °C show exclusively or mainly the α-modification. With increasing crystallization temperature the γ-modification is promoted, and at $T_c = 125$ °C the γ-modification is formed nearly exclusively.

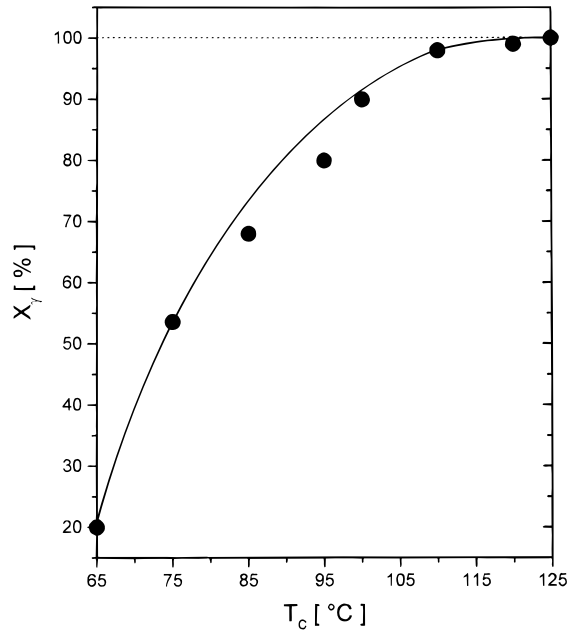

Figure 2. Content of the γ-modification as a function of the crystallization temperature.

Turner Jones showed that the amount of the γ-modification in i-PP samples containing also the α-modification, X_γ, can be calculated from the ratio of the heights of the peaks at $2\theta = 18.8°$ (h_α, 130 peak of the α-modification) and at $2\theta = 20.2°$ (h_γ, 117 peak of the γ-modification).[17] Figure 2 shows the amount of the γ-modification as a function of the crystallization tem-

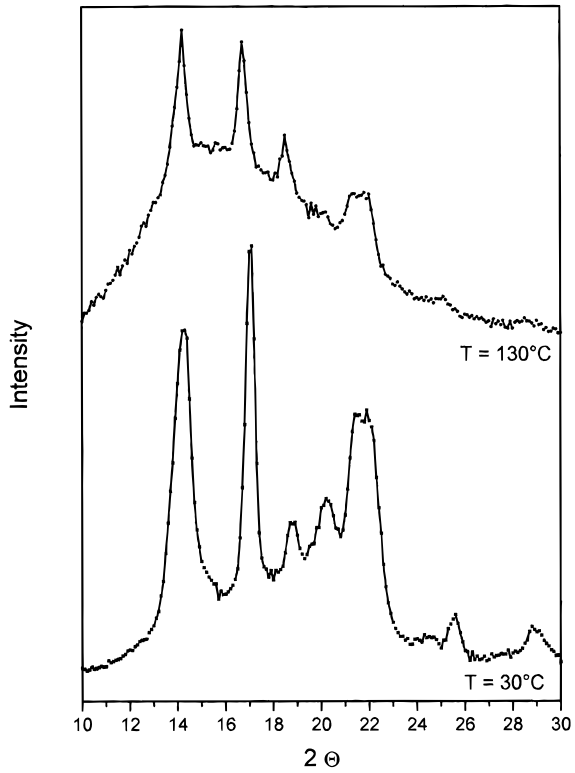

Figure 3. WAXS pattern of a sample isothermally crystallized at 75 °C: (bottom) measured at 30 °C; (top) taken after slow heating to 130 °C.

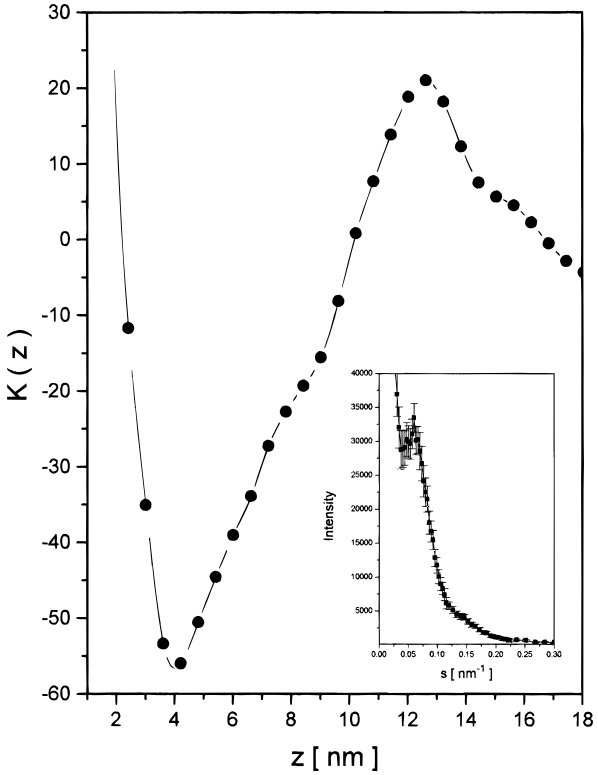

Figure 4. Correlation function $K(z)$ of the sample isothermally crystallized at 100 °C obtained by SAXS measurements. The inset shows the desmeared and corrected SAXS trace of the same sample.

perature calculated using eq 2[17,36]

$$X_\gamma = h_\gamma/(h_\gamma + h_\alpha) \qquad (2)$$

It can be seen that the γ-content of this polymer can widely be varied as a function of the crystallization temperature. At crystallization temperatures higher than 110 °C, the sample crystallizes nearly exclusively in the γ-modification. This is in agreement with calculations that the formation of the γ-modification is thermodynamically more favored compared to the α-modification.[25,26] The formation of the α-modification at larger supercoolings is thus a kinetically driven process. Therefore, the influence of the two modifications on the morphology development in this sample can be studied by simply varying the crystallization temperature. Figure 3 depicts the WAXS patterns of the i-PP sample isothermally crystallized at 75 °C. This sample is then measured after quenching to 30 °C and after slowly heating to 130 °C, respectively. Crystallization at 75 °C leads to nearly equal amounts of the α- and γ-modifications as can be seen in the sample quenched to 30 °C. During the heating of this sample to 130 °C, the γ-peak at $2\theta = 20.2°$ vanished. The α-peak at $2\theta = 18.8°$ can still be detected. Therefore, it can be assumed that the melting point of the α-modification is higher than the melting point of the γ-modification. The crystallinity disappears completely at 135 °C. In contrast, a change from the γ- to the α-modification could never be observed for all annealing regimes applied.

SAXS can be used to measure the average lamella thickness and long period of semicrystalline polymers.[37−39] The inset in Figure 4 shows the desmeared and corrected SAXS trace of the i-PP sample isothermally crystallized at 100 °C. As discussed above, the content of the γ-modification is about 90% at this crystallization temperature. The different shoulders of this curve are caused by periodic changes in the electron density of the sample connected with alternating amorphous and crystalline regions. More quantitative information can be deduced from the Fourier transformation of the scattering curve, which yields the linear correlation function $K(z)$ defined by eq 1. The position of the first minimum of the correlation function shown in Figure 4 is related to a lamella thickness of about 4 nm. The position of the first maximum of the correlation function can be assigned to the long period, which is about 12 nm. The lamella thickness of 4 nm and the long period of 12 nm are in good agreement with the crystallinity of 35% determined from the WAXS pattern using the method of Ruland[46] and with the degree of crystallinity calculated from the melting enthalpy of 72 J/g. This results in a crystallinity of 34.6% when assuming that the melting enthalpy of a 100% crystalline sample, $\Delta H_{m,100\%}$, is 209 J/g (α-modification).[41] This $\Delta H_{m,100\%}$ is used because there is only a small energy difference between the two polymorphs (α and γ), and the γ-modification appears to be at least as stable as the α-modification.[25] A lamella thickness of 4 nm fits reasonably well with the average length of isotactic chain segments of about 4.85 nm incorporated into a γ-phase lamella. The value of 4.85 nm belongs to 22.4 monomer units arranged in the 3_1 helix. Taking into consideration that the helices in the γ-modification have an angle of about 50° with respect to the lamella surface yields a lamella thickness of 3.7 nm when it is assumed that the polymer chain segments between the stereo- or regioirregularities are always packed in the crystallite. This is also in agreement with crystallization experiments of propylene copolymers, which show that relatively short isotactic polypropylene segments enhance the formation of the γ-modification.[18] The lamella thickness itself is defined by the degree of supercooling. However, in addition, the change of the crystal modifi-

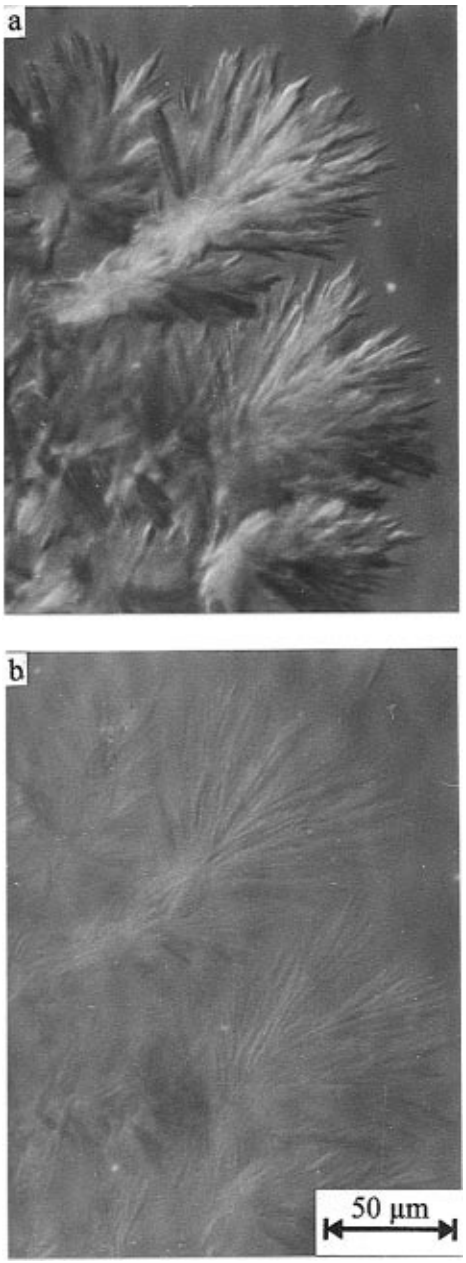

Figure 5. Phase contrast light micrographs of the i-PP sample: (a) isothermally crystallized at 110 °C for 17 min; (b) slowly heated to 132 °C.

cation can also influence the lamella thickness.[40] In the case under consideration, the length of the isotactic segments seems to promote the formation of the γ-modification. This should be caused by the fact that a thermodynamically stable lamella thickness and the average length of isotactic segments in the polymer chain packed into the γ-modification have similar numerical values in a certain temperature range.

Microscopic Observations. Figure 5 shows two, phase contrast light micrographs of the sample isothermally crystallized at 110 °C (Figure 5a) and then slowly heated to 132 °C (Figure 5b). This sample has a γ-phase content of about 98% after isothermal crystallization at 110 °C determined by WAXS. The typical morphology shown in Figure 5a will be discussed below. But the change in the morphology after heating this sample to 132 °C is interesting. Most of the crystalline material disappeared but some straight fibrils are left. These fibrils are nearly invisible compared to the morphology at 110 °C, and some photographic contrast enhancement is needed to make them clearly visible. The higher melting point of these fibrils is in agreement with the WAXS measurements discussed above. The γ-phase has a lower melting point and disappeared at 132 °C whereas the α-phase is still present. The appearance of these fibrils is similar to the formation of open spherulites in blends of normal α-phase i-PP.[42] Thus it can be concluded that there is a close connection between the formation of the α- and γ-phase influencing the morphology development of this sample.

Figure 6a shows the morphology of the sample isothermally crystallized at 125 °C for 3 days obtained by light microscopy between crossed polarizers. At this crystallization temperature the sample crystallizes nearly completely in the γ-modification. The morphologies are completely different from the well known α- or β-spherulites of i-PP. The supermolecular structure appears as single, along one axis extended entities. After a crystallization time of 3 days the sample is only partially crystallized. Some small spherulites between the extended entities are formed by nonisothermal crystallization during the cooling process. The sample isothermally crystallized at 110 °C can be seen in Figure 6b. At this crystallization temperature the content of the α-modification is slightly larger (about 2%), and this influences the morphology remarkably. These structures suggest more on bundle-like entities. The clear lateral structures are very characteristic for these bundles. It will be shown below that this lateral structure is the main morphological feature of supermolecular structures of γ-phase i-PP influenced by small amounts of crystalline material grown in the α-modification. The same sample isothermally crystallized at 85 °C (Figure 6c) shows clearly a spherulitical morphology. At this crystallization temperature the content of the α-modification is about 33%. The appearance of the three different morphologies shown in Figure 6a−c is in agreement with the WAXS measurements shown in Figure 1. The microscopic observation of the sample over a wide range of crystallization temperatures shows that with increasing content of the α-modification, the morphology changes from elongated and bundle-like entities to spherulites. The material crystallized in the α-modification initiates the lateral ongrowth of γ-phase lamellae. This ongrowth was also observed for low molecular weight i-PP.[15] For the sample isothermally crystallized at 85 °C (Figure 6c), the large amount of α-phase i-PP leads to the typical appearance of spherulites.

For comparison, Figure 7 shows the polarized light micrograph of another i-PP sample with a weight-average molecular weight of 16 000 g/mol but without irregularities (not detectable by NMR) in its polymer chain, isothermally crystallized at 132 °C. The equilibrium melting temperature of this sample determined by the method of Hoffmann and Weeks[43] is about 22 °C higher than the equilibrium melting point of the sample with the chain irregularities (T_m^0 = 181 °C compared to T_m^0 = 159 °C). The sample shows exclusively spherulites and forms the α-modification. The morphology differs from that of the sample with chain irregularities crystallized at similar degrees of supercooling (see Figure 6b). Also the crystallization of both samples (i-PP with the same molecular weight but different chain irregularities) at the same temperature leads to completely different morphologies. The material without chain irregularities shows the typical spherulite types known from higher molecular weight

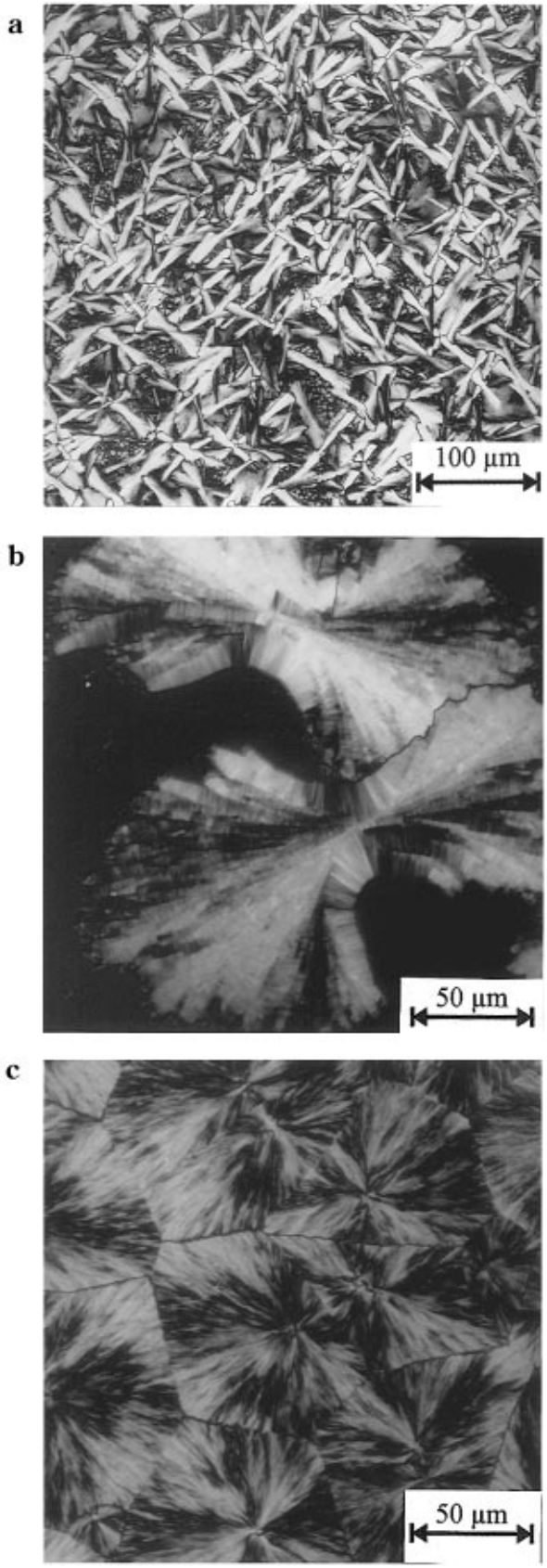

Figure 6. Polarized light micrographs of morphologies influenced by various amounts of α-phase i-PP: (a) elongated bundle-like structures in a sample crystallized at 125 °C (α-phase i-PP is hardly detected by WAXS); (b) bundle-like structures in a sample crystallized at 110 °C (2% of α-phase i-PP); (c) spherulitic structures in a sample crystallized at 85 °C (33% of α-phase material).

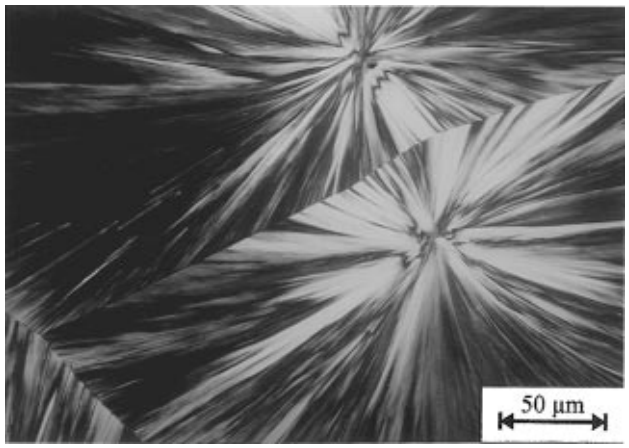

Figure 7. Polarized micrograph of an i-PP sample without stereoirregularities (M_w = 16000 g/mol) space filling crystallized in the α-modification at T_c = 132 °C.

i-PP samples.[5] Thus the distribution of the irregularities caused by the polymerization mechanism dominates the resulting morphologies.

AFM is able to provide more detailed information on the crystalline morphologies. Figure 8a shows an AFM micrograph of the sample with chain irregularities crystallized at 85 °C (the light micrograph of this sample is depicted in Figure 6c). The morphology is spherulitic, caused by the composition of the sample which contains 33% of α-phase i-PP. The impingement lines of the spherulites can clearly be seen. The higher magnification of this morphology shown in Figure 8b indicates that these entities are formed by the lateral ongrowth of the γ-phase on the α-phase. The morphology of the sample crystallized at 125 °C can be seen in Figure 8c. At this temperature the sample crystallizes nearly completely in the γ-modification as shown by WAXS measurements, but again the typical lateral ongrowth is clearly visible, indicating that a certain amount of α-phase i-PP must be formed. Both modifications together result in the morphological appearance shown in the light micrograph of Figure 6a. The tips of an elongated bundle-like structure of the sample isothermally crystallized at 130 °C show an interwoven morphology (Figure 8d). Straight entities appear similar to strings of pearls. They are frequently arranged in an angle of about 80° to each other. This angle is typical for homoepitaxial growth of α-phase i-PP and is commonly called "crosshatching".[5] This suggests that the interwoven morphology is formed by γ-phase ongrowth on crosshatched α-phase i-PP. The three-dimensional image of an enlarged area of this sample can be seen in Figure 8e. The γ ongrowth is now clearly visible and has the typical triangular appearance as discussed by Lotz et al. for low molecular weight samples.[15] This morphology of the γ ongrowth on crosshatched α-phase i-PP is most typical for crystallization temperatures above 120 °C.

The kinetics of the crystallization process is observed by relative light intensity measurements. Figure 9 shows a measurement of the relative light intensity between crossed polarizers of the sample during the isothermal crystallization at 120 °C. The inset shows for comparison the time dependence of the relative light intensity of an i-PP sample crystallizing completely in the α-modification. The trace in the inset shows clearly that the 50% value of the relative light intensity corresponds well with the crystallization half time. For the polymer crystallizing mainly in the γ-modification,

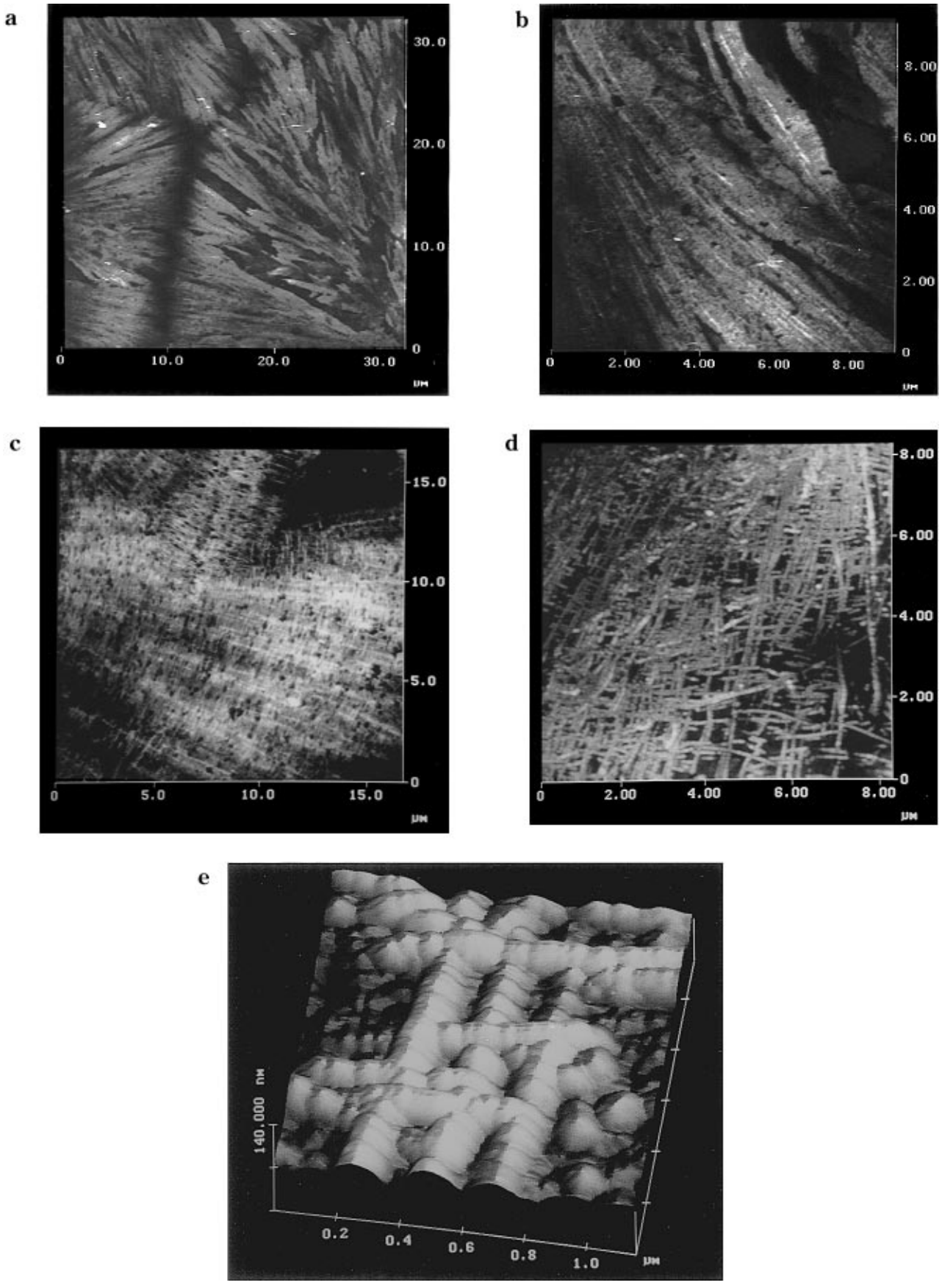

Figure 8. AFM micrographs of the sample isothermally crystallized at different temperatures: (a) 85 °C; (b) as (a) but enlarged; (c) 125 °C; (d) 130 °C; (e) three- dimensional image of an enlarged area of (d).

the situation is different. The 50% value of the relative light intensity is reached in an early state of the crystallization process (after about 4 h). This is far less than the crystallization half time. This behavior can be explained with the morphology development during the crystallization process of the γ-phase-rich material. Figure 10 shows four polarized light micrographs taken after crystallization times indicated by arrows in Figure

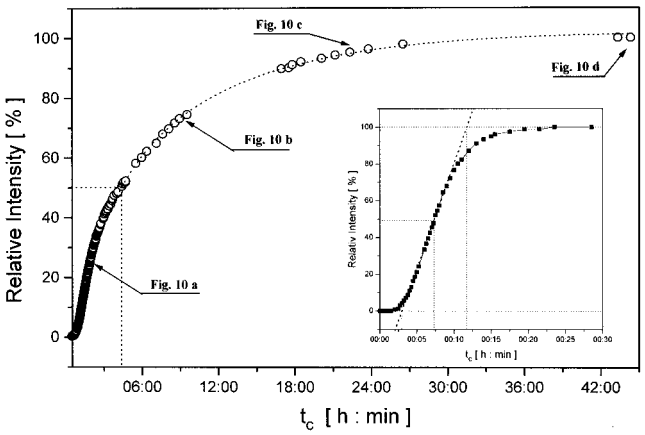

Figure 9. Relative light intensity observed during the isothermal crystallization at 120 °C. The inset shows the relative light intensity for a polymer crystallizing exclusively in the α-modification (M_w = 248 000 g/mol, T_c = 120 °C).

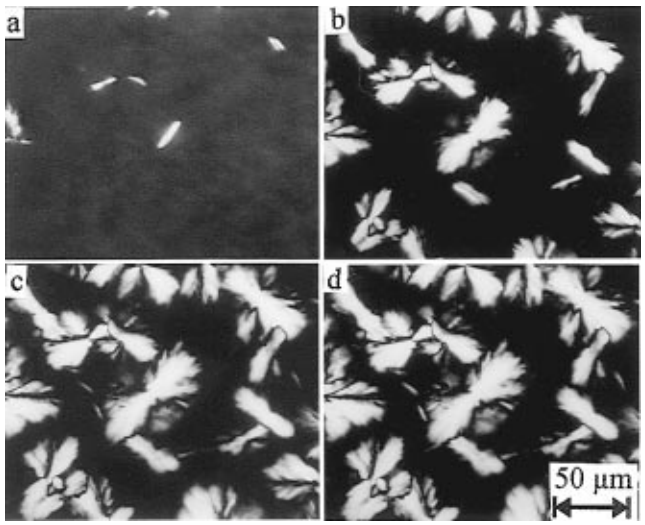

Figure 10. Polarized light micrographs taken during isothermal crystallization at 120 °C after different crystallization times indicated by arrows in Figure 9: (a) 1:50 h; (b) 4:30 h; (c) 23 h; (d) 43 h.

9. The micrograph taken at t_c = 1:50 h (Figure 10a) shows elongated entities that are typical for the early stage of crystallization of α-phase lathes with γ-phase ongrowth similar to that reported for low molecular weight samples.[15] The micrograph taken at t_c = 4:30 h (Figure 10b) shows more bundle-like entities. The micrographs taken after 23 and 43 h (Figure 10c,d) do not show any significant difference, indicating that the growth of the bundle-like entities is finished long before the bundles become space filling. After that, only diffuse structures between the needle-like entities appear not visible in the polarized light micrographs. As will be shown below, the dark areas contain also crystalline material. This is crystallized completely in the γ-modification without any contributions of the α-modification. Because there are two competing crystallization processes, the 50% value of the relative light intensity does not correspond to the crystallization half time. Figure 11a shows an AFM measurement of the sample isothermally crystallized at 120 °C for 96 h. The elongated structures correspond to the bundle-like entities observed by polarized light microscopy (see Figure 10). Figure 11b shows the morphology of the crystalline material formed in the dark areas of Figure 10d. In this area, a network structure appears that is different from the elongated bundles. A closer look at these

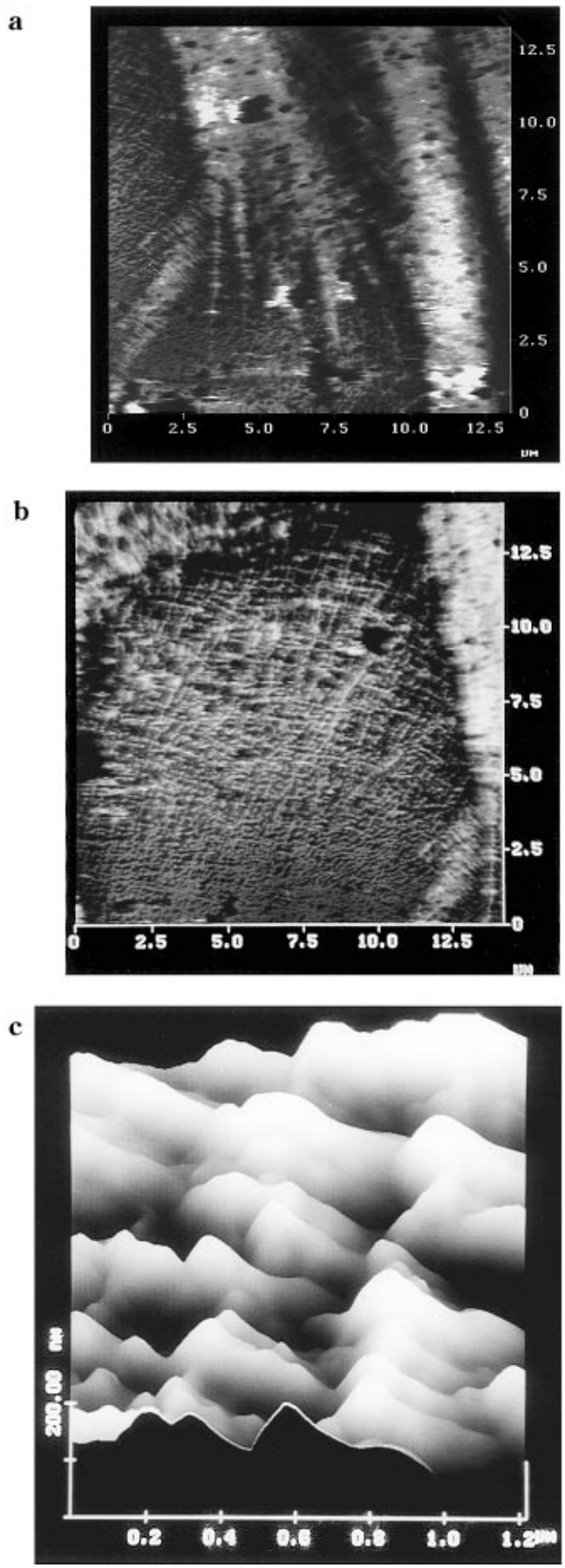

Figure 11. AFM micrograph of a sample isothermally crystallized at 120 °C: (a) an elongated morphology; (b) large-scale image of a network structure of crystalline entities; (c) three-dimensional image of an enlarged area of (b).

structures (Figure 11c) shows parallel slices which have on top a triangular appearance. This is very similar to single crystals developed by the γ-phase of i-PP after growing on α-phase lathes as discussed by Lotz et al.[15] It therefore seems possible that this structure is formed by single-crystal-like aggregates. However, it can be excluded that this is a γ-phase ongrowth on the α-phase for two reasons. In the case that the γ-phase ongrowth occurs on single lathes of the α-phase, all triangles are arranged in straight lines (see Figure 15b). In the case that the α-phase has extensive crosshatching, the triangles are arranged in an angle of 80° to each other as shown in Figure 8e.

Figure 12 shows an etched bulk sample after a slow cooling process from the melt at 160 °C to the isothermal crystallization temperature of 120 °C. For the etching process, the free surface of the sample to vacuum is used in order to avoid any artifacts which may be caused by induced crystallization when the sample is in contact with substrates as e.g. epitaxial growth. The photograph in Figure 12a depicts columns with a rectangular cross-section. There are well-ordered extended crystalline entities. These entities have very sharp boundaries and thus appear single-crystal-like. Figure 12b shows an enlarged area of the columns. The small regular structure in the upper left corner is an artifact caused by AFM measurements. Figure 12c represents the corresponding height profile measured along the diagonal of the micrograph and perpendicular to the steps. The steps between the arrows indicated in Figure 12c have a height of about 50−60 nm or multiples of this value. The chain length of the polymer used in its 3_1 helix is 58 nm. Packing these helices into lamellae of the γ-modification would yield a thickness of about 45 nm, assuming that extended chains are always packed into lamellae with an angle of 50° to the surface. Taking into consideration that there is a distribution in chain length, these data agree fairly well in order to conclude that the columns shown represent extended-chain γ lamellae. The occurrence of extended-chain lamellae induced by applying pressure or slow cooling from the melt has been reported for several other polymers.[40,45] For the polymer under investigation, a change from chain-folded crystallization to extended-chain crystallization occurs obviously with increasing crystallization temperature. This phenomenon is not completely understood. The main reason might be the temperature dependence of the lamella thickness. The packing of isotactic chain segments into these chain-folded lamellae is only favored for a certain temperature interval. At low supercoolings the lamella thickness increases and the number of isotactic segments which fit into these lamellae decreases. The result is an extended-chain crystallization.

AFM is a remarkable tool to study surfaces of crystalline polymers on a molecular scale. As can be seen in Figure 12b, the flat-on surface of the columns is very smooth and provides the opportunity to scan this area by AFM with a molecular resolution as shown in Figure 13a. The methyl groups appear as bright rows parallel to the column direction. This direction is simultaneously parallel to the double-packed layers of helices and thus parallel to the edge-on surface of the extended-chain lamellae. Figure 13b presents additionally to the AFM micrograph the schematic direction of the methyl group rows in the (010) plane which are arranged parallel to the stripes according to the model of Brückner and Meille. The visible area of the micrograph

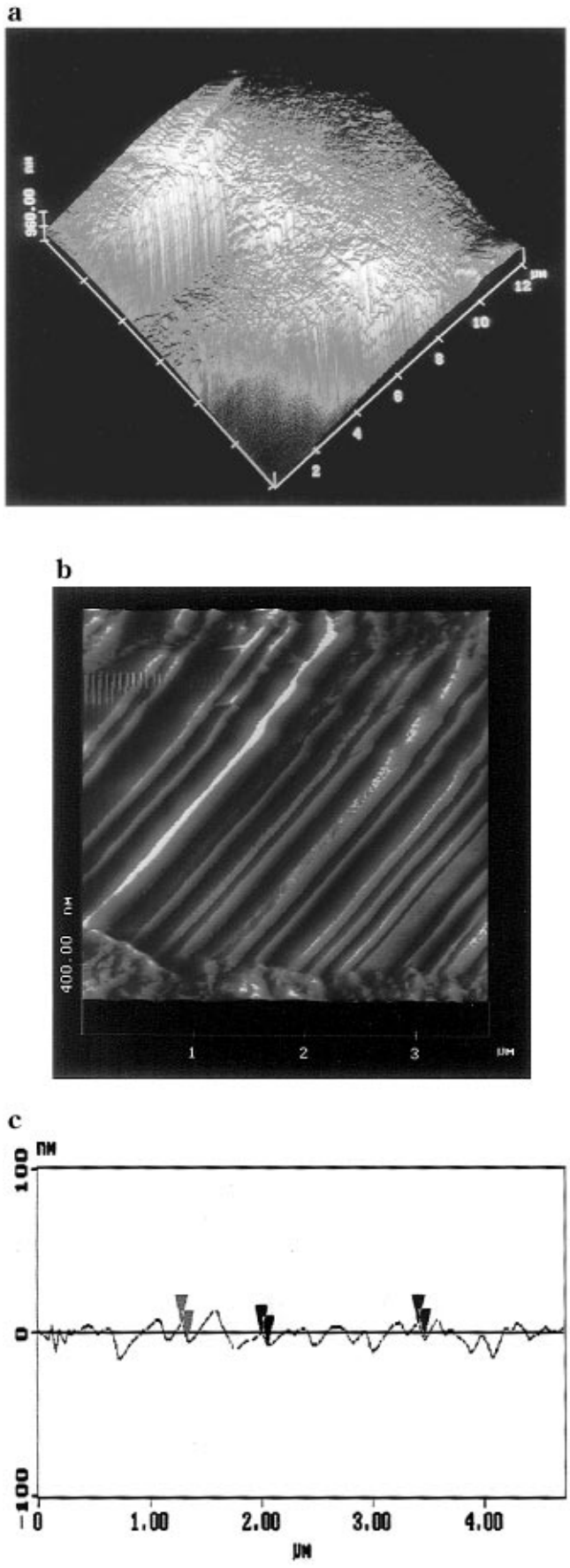

Figure 12. Crystalline morphology of γ-phase i-PP in the bulk sample (T_c = 120 °C) observed by AFM: (a) columns with a rectangular cross-section; (b) enlarged area of (a); (c) height profile taken perpendicular to the steps at the diagonal.

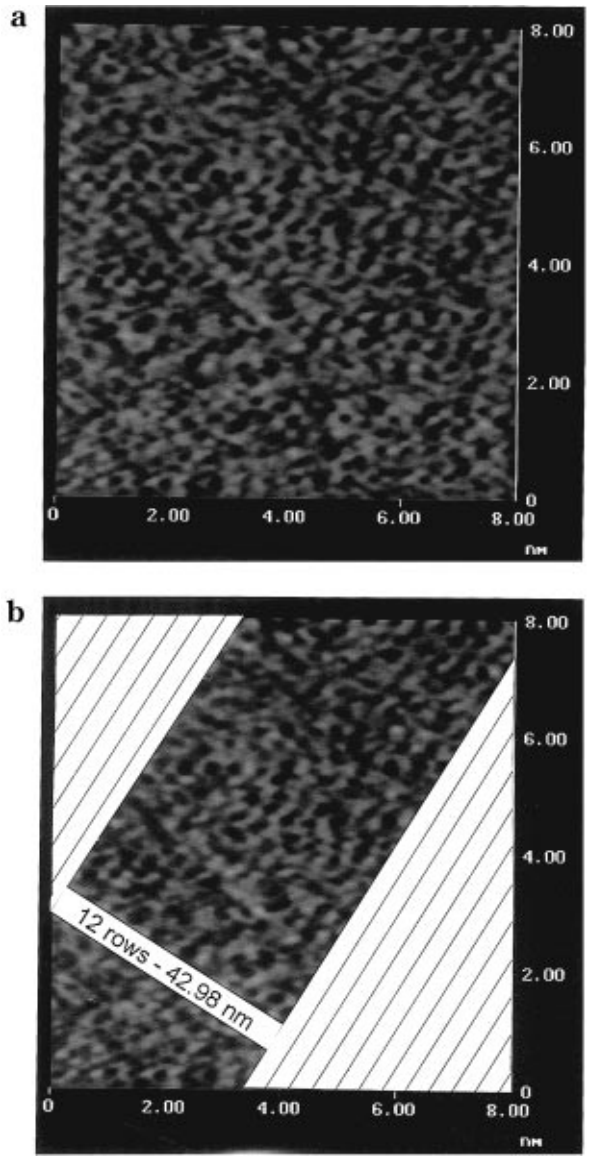

Figure 13. High-resolution AFM images of the columns taken at the flat-on surface (010): (a) molecular resolution showing methyl groups; (b) the lines represent the direction of methyl group rows.

contains exactly 12 rows of methyl groups. The number of rows is determined by several height profiles taken perpendicular to the lines. The overall spacing is about 43 Å; i.e. the spacing between the methyl group rows is 3.6 Å. The methyl groups are apparently not very well ordered. However, this has to be expected as can be seen in the schematic drawing of the crystalline arrangement of γ-phase i-PP shown in Figure 14. The double-packed helices arranged in an angle of 80° to each other can be seen in the (110) plane. The area scanned with a molecular resolution by AFM and depicted in Figure 13b lies on the (010) plane. It is already obvious that the plane scanned by AFM does not have a very regular order of the methyl groups. Because of the tilting of the double-packed helices, the methyl groups appear somewhat irregular. They are shown as open dots on the (010) surface in the schematic drawing. This schematic drawing also shows the periodic distance of methyl group rows of 3.53 Å calculated from the crystallographic data, which is in good agreement with the value of 3.6 Å obtained by AFM.

Under the experimental conditions described, a broad variety of crystalline morphologies is obtained. Therefore, we tried to prepare single crystals by thermal annealing of crystalline entities prepared from diluted solutions. The i-PP aggregates on the glass surface are molten and then slowly cooled to the crystallization temperature of 120 °C. The resulting morphology can be seen in Figure 15a. This AFM measurement reveals that the single-crystal aggregates are formed by stacks of triangular slices. Again the thickness of the single crystals corresponds approximately to the length of extended chains packed into lamellae formed by the γ-phase. Figure 15b can be used to demonstrate the difference when the formation of these single crystals is influenced by the α-phase. The single-crystal aggregate shown in Figure 15b depicts also a kind of triangular slices but arranged in two rows along one valley in the middle part. This is exactly the appearance of γ-phase ongrowth on α-phase i-PP discussed by Lotz et al.[15]

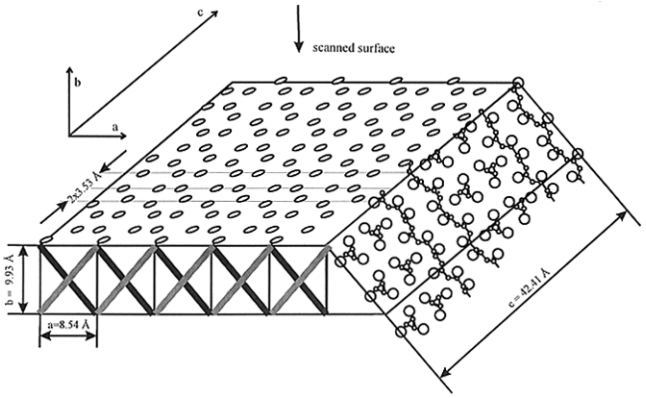

Figure 14. Schematic drawing of the crystal lattice with dimensions and the arrangement of helices in the (110) plane of the γ-phase.

Conclusions

Metallocene/MAO catalyst systems are able to produce i-PP samples with well-defined stereo- and regioirregularities. These irregularities can be used to tailor the crystalline morphology of i-PP samples. Thus it is possible for the first time to produce a relatively high molecular weight i-PP sample which forms almost completely the γ-modification. The content of the γ-modification can be controlled via the crystallization temperature. The γ-phase crystallizes preferably at low supercoolings whereas the formation of the α-phase is favored at higher supercoolings as demonstrated by WAXS measurements. Even in the case that the sample forms nearly completely the γ-modification, the morphology development is widely influenced by very small amounts of α-phase i-PP. The γ-phase ongrowth on α-phase lamellae is most typical for the supermolecular structure formation. i-PP samples containing a large amount of γ-phase material form mainly bundle-like structures. Larger amounts of α-phase i-PP lead to spherulitic morphologies but even in this case AFM is able to show that γ-phase ongrowth on α-phase lamellae occurs. SAXS shows a small lamella thickness of about 4 nm for γ-phase i-PP crystallized at 100 °C. This lamella thickness corresponds to the average length of isotactic chain segments of this sample packed into lamellae of γ-phase i-PP. The long period is about 12 nm. At higher crystallization temperatures crystallization without any influence of α-phase i-PP could be observed. In the bulk, columns of γ-phase i-PP with a rectangular cross-section are formed at low super-

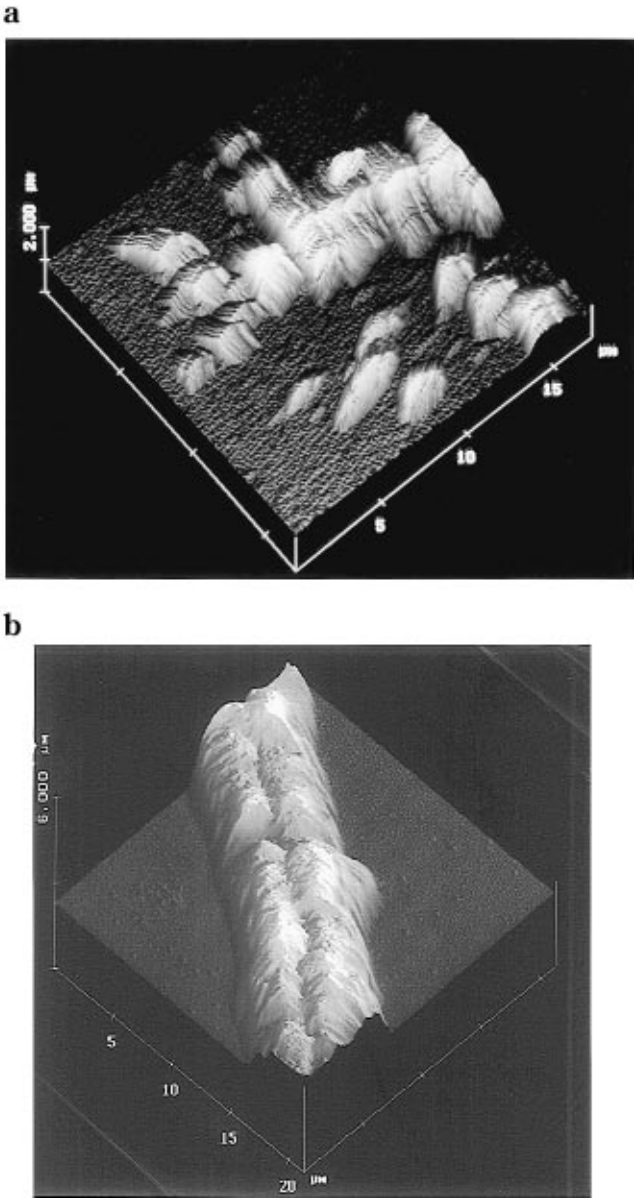

Figure 15. (a) Aggregates of single crystals formed by extended chains of γ-phase i-PP on glass of solvent-cast samples, which were molten and isothermally crystallized at 120 °C (without etching). (b) For comparison, the γ-phase ongrowth on α-phase i-PP lathes (same crystallization conditions as (a)).

coolings. It is also possible to prepare single crystals with a triangular shape. The columns as well as the single crystals are formed by extended chains. AFM measurements show a distance of methyl group rows on the (010) surface of the columns of 3.6 Å, which is in good agreement with the theoretical value of 3.53 Å.

Acknowledgment. We gratefully acknowledge the synthetic support by Dr. D. Fischer, who supplied the i-PP samples. B. Heck carried out the SAXS measurement. This work was supported by the Bundesministerium für Bildung und Forschung (project #03M40719).

References and Notes

(1) Khoury, H. *J. Res. Natl. Bur. Stand. Sect. A* **1966**, *70A*, 29.
(2) Padden, F. J.; Keith, H. D. *J. Appl. Phys.* **1966**, *37*, 4013.
(3) Padden, F. J.; Keith, H. D. *J. Appl. Phys.* **1973**, *44*, 1217.
(4) Basset, D. C.; Olley, R. H. *Polymer* **1984**, *25*, 935.
(5) Norton, D. R.; Keller, A. *Polymer* **1985**, *26*, 704.
(6) Brückner, S.; Meille, S. V.; Petraccone, V.; Pirozzi, B. *Prog. Polym. Sci.* **1991**, *16*, 361.
(7) Lotz, B.; Wittmann, J. C. *Prog. Colloid Polym. Sci.* **1992**, *87*, 3.
(8) Turner Jones, A.; Aizlewood, J. M.; Beckett, D. R. *Makromol. Chem.* **1964**, *75*, 134.
(9) Kardos, J. L.; Christiansen, E.; Baer, E. *J. Polym. Sci., Part A-2: Polym. Chem.* **1966**, *4*, 777.
(10) Pae, K. D.; Morrow, D. R.; Sauer, J. A. *Nature* **1966**, *211*, 514.
(11) Lotz, B.; Graff, S.; Wittmann, J. C. *J. Polym. Sci., Part B: Polym. Phys.* **1986**, *24*, 2017.
(12) Morrow, D. R.; Newman, B. A. *J. Appl. Phys.* **1968**, *39*, 4944.
(13) Kojima, M. *J. Polym. Sci., Part B* **1967**, *5*, 245.
(14) Kojima, M. *J. Polym. Sci., Part A-2* **1968**, *6*, 1255.
(15) Lotz, B.; Graff, S.; Straupé, C.; Wittmann, J. C. *Polymer* **1991**, *32*, 2902.
(16) Awaya, H. *J. Polym. Sci., Polym. Lett. Ed.* **1966**, *4*, 127.
(17) Turner Jones, A. *Polymer* **1971**, *12*, 487.
(18) Giuidetti, G. P.; Busi, P.; Giulianetti, I.; Zanetti, R. *Eur. Polym. J.* **1983**, *19*, 757.
(19) Busico, V.; Corradini, P.; De Rosa, C.; Di Benedetto, E. *Eur. Polym. J.* **1985**, *21*, 239.
(20) Avella, M.; Martuscelli, E.; Della Volpe, G.; Segre, A.; Rossi, E.; Simonazzi, T. *Makromol. Chem.* **1986**, *187*, 1927.
(21) Marigo, A.; Marega, C.; Zanetti, R.; Paganetto, E.; Canossa, E.; Coleta, F.; Gottardi, F. *Makromol. Chem.* **1989**, *190*, 2805.
(22) Mezghani, K.; Phillips, P. J. *Polymer* **1995**, *35*, 2407.
(23) Fischer, D.; Mülhaupt, R. *Makromol. Chem. Phys.* **1994**, *195*, 1143.
(24) Jüngling, S. Ph.D. Thesis, Freiburg, 1995.
(25) Ferro, D. R.; Brückner, S.; Meille, S. V.; Ragizzi, M. *Macromolecules* **1992**, *25*, 5231.
(26) Meille, S. V.; Ferro, D. R.; Brückner, S. *Polym. Prepr. (Am. Chem. Soc., Div. Polym. Chem.)* **1992**, *33* (1), 268.
(27) Brückner, S.; Meille, S. V. *Nature* **1989**, *340*, 455.
(28) Meille, S. V.; Brückner, S.; Porzio, W. *Macromolecules* **1990**, *23*, 4114.
(29) Brückner, S.; Meille, P.; Sozzani, P.; Torri, G. *Makromol. Chem., Rapid Commun.* **1990**, *11*, 55.
(30) Turner, J. D.; Lingafelter, E. C. *Acta Crystallogr.* **1955**, *8*, 551.
(31) Fischer, D. Ph.D. Thesis, Freiburg, 1992.
(32) Strobl, G. R. *Acta Crystallogr.* **1970**, *A26*, 367.
(33) Russell, T. P.; Ito, H.; Wignall, G. D. *Macromolecules* **1988**, *21*, 1703.
(34) Strobl, G. R.; Schneider, M. J.; Voigt-Martin, I. G. *J. Polym. Sci., Part B: Polym. Phys.* **1980**, *18*, 1361.
(35) Tanabe, Y.; Strobl, G. R.; Fischer, E. W. *Polymer* **1986**, *27*, 1147.
(36) Rieger, B.; Mu, X.; Mallin, D. T.; Rausch, M. D.; Chien, J. C. W. *Macromolecules* **1990**, *23*, 3559.
(37) Morrison, J. D.; Burgess, A. N.; Stephensen, R. C. *Polymer* **1994**, *35*, 2272.
(38) O'Kane, W. J.; Young, R. J.; Ryan, A. J.; Bras, W.; Derbyshire, G. E.; Maut, G. R. *Polymer* **1994**, *35*, 1352.
(39) Thomann, R.; Kressler, J.; Setz, S.; Wang, C.; Mülhaupt, R. *Polymer* **1996**, *37*, 2627.
(40) Wunderlich, B. *Macromolecular Physics*; Academic Press: New York, 1973; Vol. 1.
(41) Quirck, R. P.; Ajsamarraie, M. A. A. *Polymer Handbook;* J. Wiley & Sons: New York, 1989.
(42) Lim, G. B. A.; Lloyd, D. R. *Polym. Eng. Sci.* **1993**, *33*, 513.
(43) Hoffmann, J. D.; Weeks, J. J. *J. Res. Natl. Bur. Stand., Sect. A* **1962**, *66A*, 13.
(44) Natta, G.; Corradini, P.; Cesari, M. *R. C. Accad. Lincei* **1956**, *21*, 365.
(45) Rastogi, S.; Ungar, G. *Macromolecules* **1992**, *25*, 1445.
(46) Ruland, W. *Acta Crystallogr.* **1961**, *14*, 1180.

MA951885F